Zeeman effect

This is a long evaluation for the experiment "F44: Zeeman effect" as part of the advanced lab at the University of Heidelberg
winter semester 2018/2019

A. Matthes

January 25, 2019

Contents

1 Introduction and theory **3**

2 PART I: Observing the Zeeman effect and measuring the Bohr magneton μ_B **6**

2.1 Setup 6

2.2 Hysteresis 6

2.3 Cd spectrum 8

2.3.1 Transversal 8

2.3.2 Longitudinal 10

2.4 Measuring the Bohr magneton μ_B 12

3 PART II: Precision spectroscopy **15**

3.1 Setup 15

3.2 Dispersion function of the spectrometer 15

3.3 Cadmium line 17

3.4 Neon spectrum 17

4 Discussion and Conclusion **18**

4.1 Discussion of Part I 18

4.2 Discussion of Part II 19

4.3 Conclusion 20

1 Introduction and theory

Cadmium has atomic number 48 which gives it the electron configuration $[Kr]4d^{10}5s^2$. So in its fifth shell the total spin quantum number is $S = 0$. We will be investigating the transition $5^1D_2 \rightarrow 5^1P_1$ to confirm some predictions about energy level splitting that arise in atomic physics. We will also try to determine the wavelength of the corresponding spectral line.

Quantum theory predicts that (for $S = 0$) an energy level for some orbital angular momentum quantum number L is actually composed of $L(L+1)$ degenerate energy levels that can be distinguished by the quantum number M_L (here also just M since there is no risk of confusing it with M_S for the spin). It can have values $-L \leq M_L \leq +L$. M_L and L are defined such that $\hbar^2 L(L+1)$ is the eigenvalue of the squared angular momentum operator $\hat{L}^2$ and $\hbar M_L$ is the eigenvalue of the operator for the projection of the angular momentum on some specific axis $\hat{L}_z$.
A charged particle with some angular momentum $\vec{J}$ has a magnetic moment

$$\vec{\mu} = g\frac{q}{2m}\vec{J} \tag{1}$$

where q is the charge of the particle, m is its mass and g is the g-factor whose value depends on the kind of angular momentum and kind of particle involved. Today we are only interested in the case of electrons with $S = 0$, so $\vec{J} = \vec{L}$, $q = -e$, $m = m_e$ and $g = g_{e,l} = 1$. We can rewrite (1) as

$$\vec{\mu} = -\frac{\mu_B}{\hbar}\vec{L} \tag{2}$$

$\mu_B = \frac{e\hbar}{2m}$ is the **Bohr magneton**. One goal of this experiment is to find its value.
In a magnetic field $\vec{B}$ a magnetic moment $\vec{\mu}$ will have potential energy

$$E_{pot} = -\vec{\mu} \cdot \vec{B} \tag{3}$$

Using (2) and setting the z-axis along the magnetic field lines, so that $|B| = |B_z| = B$ and using $|L_z| = \hbar M_L$ we can expand that to

$$E_{pot} = \frac{\mu_B}{\hbar}\vec{L} \cdot \vec{B} = \mu_B M_L B \tag{4}$$

Let us consider what this means for the subshell $^1P_2$. Here $L = 1$, so $M_L \in \{-1, 0, +1\}$. Without an external magnetic field[1] these will all have the same energy.

[1]The magnetic field induced by the relative motion of the charged nucleus also causes some

But if we introduce a magnetic field the potential energy in (4) will "pull apart" those degeneracies into three different energy levels. Similarly, the $^1D_2$ level will be split up into five such levels. This is the **Normal Zeeman Effect**.

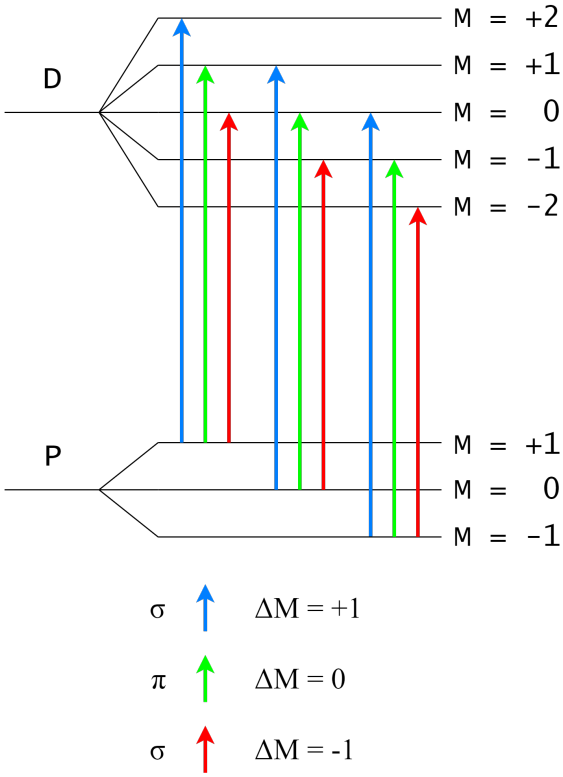

Figure 1: Energy level splitting of 5^1D_2 and 5^1P_1 that create the Zeeman splitting of the red cadmium line at 644nm.

Figure 1 shows how one can visualise this splitting. Notice that the energy shift between two neighbouring sub-energy levels does not depend on L.
Another prediction of quantum mechanics is about which transitions between these levels are allowed. These **selection rules** are a result of conservation of angular momentum and parity[2]. By evaluating the transition dipole moment one can show that a transition from a state a to a state b can only happen, if

$$\Delta M_J = M_{J,a} - M_{J,b} = 0, \pm 1$$

$$\Delta L = L_a - L_b = \pm 1$$

and

$$\Delta S = 0$$

In our case ($5^1D_2 \to 5^1P_1$) $\Delta L = 1$ and $\Delta S = 0$. So we only need to worry about $\Delta M_J = \Delta M_L$. Figure 1 demonstrates what this means for the possible transitions. We find that there are only three transitions whose energy E is distinct. This means that we will only see three distinct spectral lines with wavelengths

$$\lambda_\pi = \frac{hc}{E} \quad \text{and} \quad \lambda_{\sigma\pm} = \frac{hc}{E \pm \Delta E} \tag{5}$$

where $\Delta E = \mu_B B$ (see (4) and note that M only changes by one) and E is the energy difference of 5^1D_2 and 5^1P_1 (without the splitting).
The transition dipole moment also tells us about what polarisation the emitted pho-

splitting. This however, is beyond the accuracy of this experiment

[2]While parity conservation is violated in weak interactions, it does hold in electromagnetism which is the dominant force here.

ton will have. It turns out that when viewing perpendicular to the magnetic field lines the light will be linearly polarised for both $\Delta M = 0$ (so called π transitions) and for $\Delta M = \pm 1$ (σ transitions) but in different directions. When viewing along the magnetic field lines, the π line will vanish and the σ lines will be circularly polarised (in opposite directions).

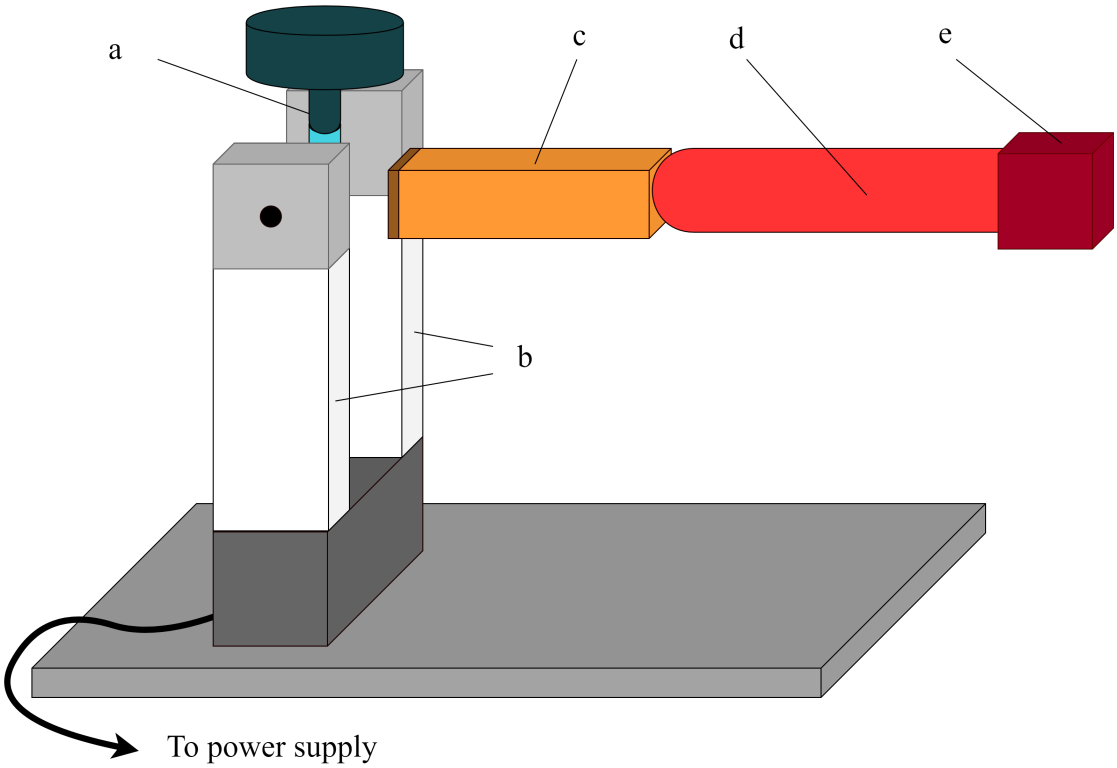

Figure 2: Simplified experimental setup. a) Cadmium lamp b) Electromagnet coils with pole pieces c) Red light filter and Lummer-Gehrcke plate d) Telescope e) Camera

2 PART I: Observing the Zeeman effect and measuring the Bohr magneton μ_B

2.1 Setup

Figure 2 shows our main experimental setup for this part. We use an electromagnet to create a magnetic field into which we place a cadmium lamp. To observe the splitting of the red line that we are interested in, we use a red filter and a Lummer-Gehrcke plate. The resolution of our camera (and our eyes) is limited, so the setup also includes a small telescope.

2.2 Hysteresis

We control the magnetic field at the location of the cadmium lamp via the current in the electromagnets. Naively, we might expect that the magnetic field B grows linear with the current in the coils I because we know the magnetic field in a coil is given by $B = \mu n I$, where n is the number of turns per unit length. However, our electromagnet uses metallic pole pieces to channel the uniform magnetic field to the

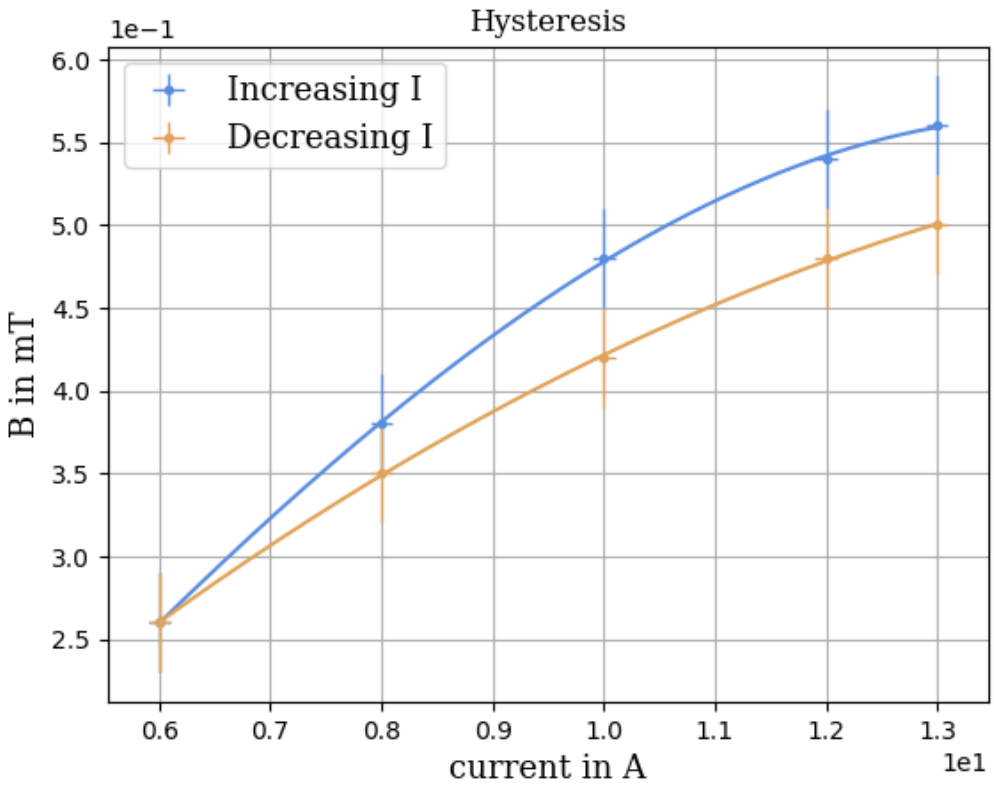

Figure 3: Hysteresis in our magnetic cores

cadmium lamp (see figure 2) and those cores exhibit hysteresis effects. This means that B can depend on the recent history of the magnetic field in the cores.
To observe the relevance of this effect for later measurements, we used a Hall probe to measure B as a function of I at the location where the lamp will be in our later measurements. We do this twice. One time, we start at $I = 13A$ and work our way down to $I = 6A$ and the other time, we *increase* the current between measurements. Figure 3 shows our results.
We do consistently measure a stronger field at the same current when we are increasing I. This indicates that there is some hysteresis happening. However, the differences are not that high ($< 15\%$ and $< 2\sigma$). If we simply take the average value for B at each current, we can fit a linear function to the data. Figure 4 shows this approach. We observe that our fit describes the data well and is adequate for our accuracy.

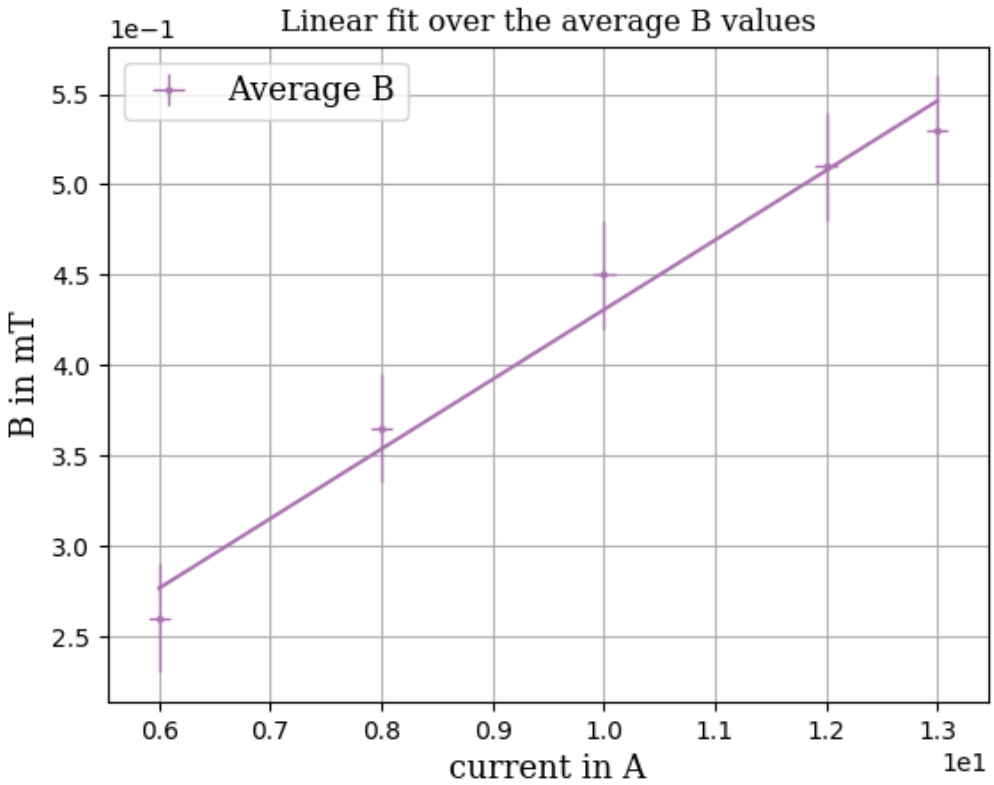

Figure 4: Average $B(I)$ dependence. Our fit function was $B = a * I + b$ and we found $a = (0.039 \pm 0.003)mT/A$ and $b = (0.05 \pm 0.03)mT$

2.3 Cd spectrum

2.3.1 Transversal

We now reinsert the cadmium lamp and take spectra at different currents to observe the effect that the magnetic field strength B has on the spectral lines.
Without the magnetic field, we only see one spectral line, (the many lines in the picture are just many diffraction orders of the same line) but when we turn on a magnetic field, this line splits into three. Figure 5 shows this.
The theory behind the normal Zeeman effect tells us that the energy splitting increases as B increases ($\Delta E = \mu_B m_l B$) which would result in a bigger separation of the lines. This is indeed what we observe, as seen in figure 6.
This measurement also tells us about the quality of data that we can expect in the coming parts of this experiment. We find that our camera has lots of dead pixels and that the resolution is quite low. We can also see that there is a lot of other scattered light. This may be due to smudges and scratches on the optical equipment. As a result of all these problems there are only a couple of refraction orders where the

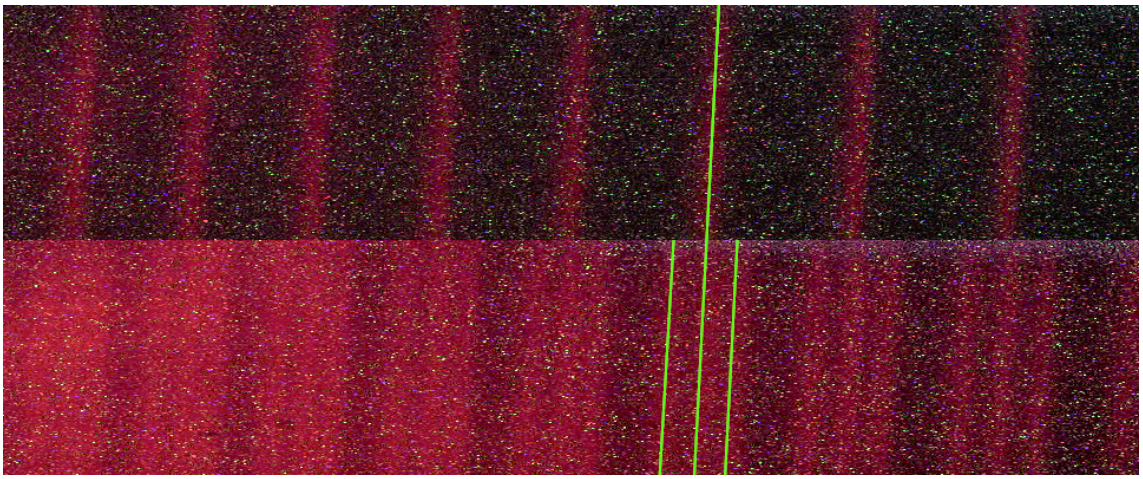

Figure 5: Spectrum without (top) and with (bottom) a magnetic field

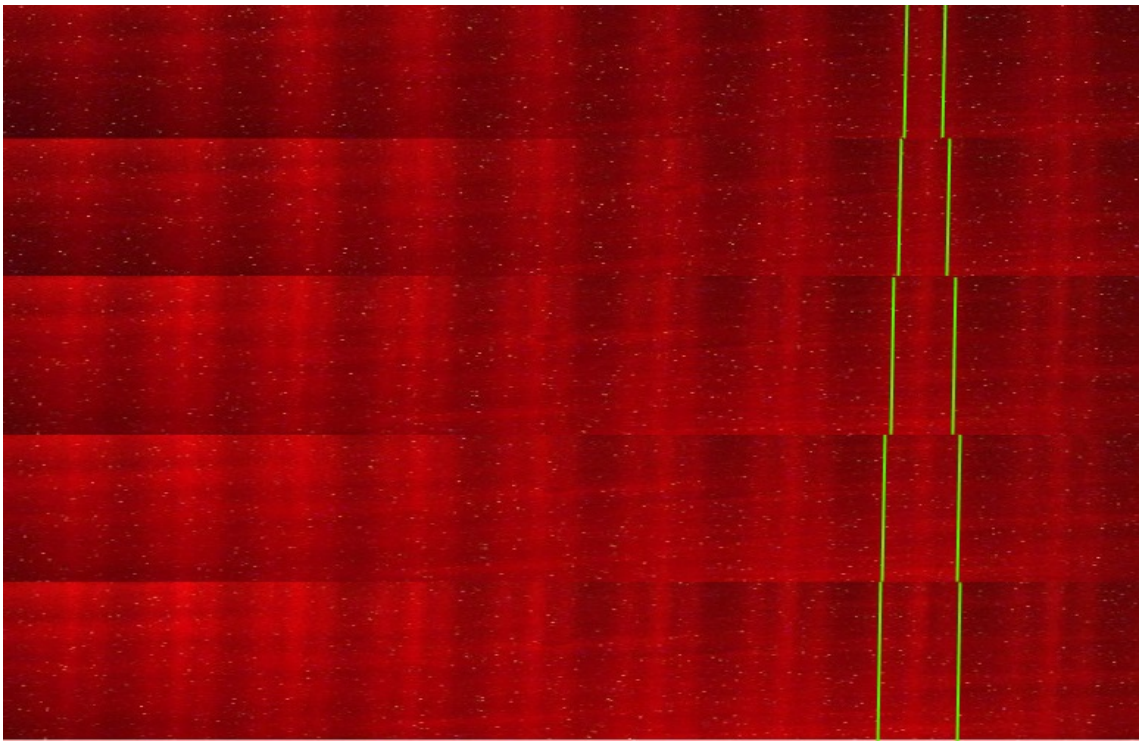

Figure 6: Transversal spectrum for $I = 8A, 9A, 10A, 11A$ and $12A$ (top to bottom)

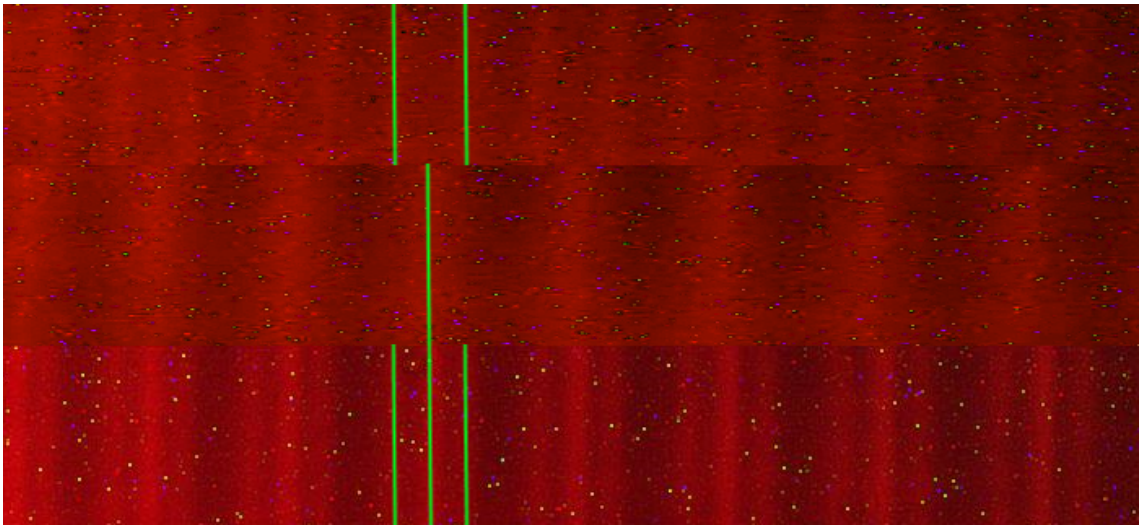

Figure 7: The effect of applying a linear polarisation filter to the transversal spectrum. The filter was turned 90° between the first two pictures

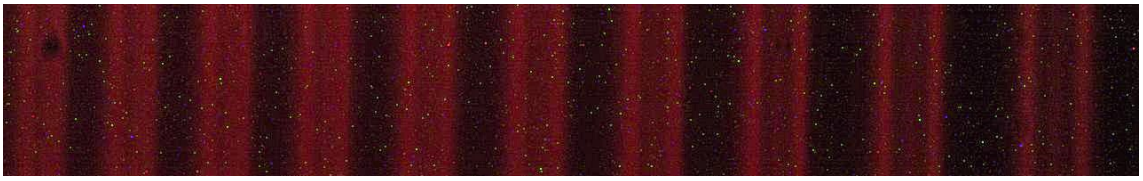

Figure 8: The longitudinal spectrum without any filters at 12A

line splitting can be clearly observed, even at $12A$.
We expect that, in transverse direction, we only observe linearly polarised light. We can test that theory by using a linear polarisation filter on the light. Figure 7 shows that this is indeed the case. By turning the filter we can either filter out the middle line ($\Delta m = 0$ and polarisation direction of the filter perpendicular to the magnetic field) or the outer ones ($\Delta m = \pm 1$ and polarisation parallel to the magnetic field).

2.3.2 Longitudinal

By turning the magnets we can observe the spectrum **along** the magnetic field lines as well. This time we only expect to find the circularly polarised light of the σ lines. Figure 8 shows the longitudinal spectrum at $I = 12A$. We indeed do lose the π line in the middle. To verify the polarisation of the σ lines we use a $\lambda/4$ waveplate to turn the circularly polarised light into linearly polarised light which we can identify with the linear polarisation filter as above.
We can tell the linear polarisation filter apart from the $\lambda/4$ waveplate by holding them against the computer monitor and turning them. At some angles the linear polarisation filter will barely let any monitor light through. This is because LCD

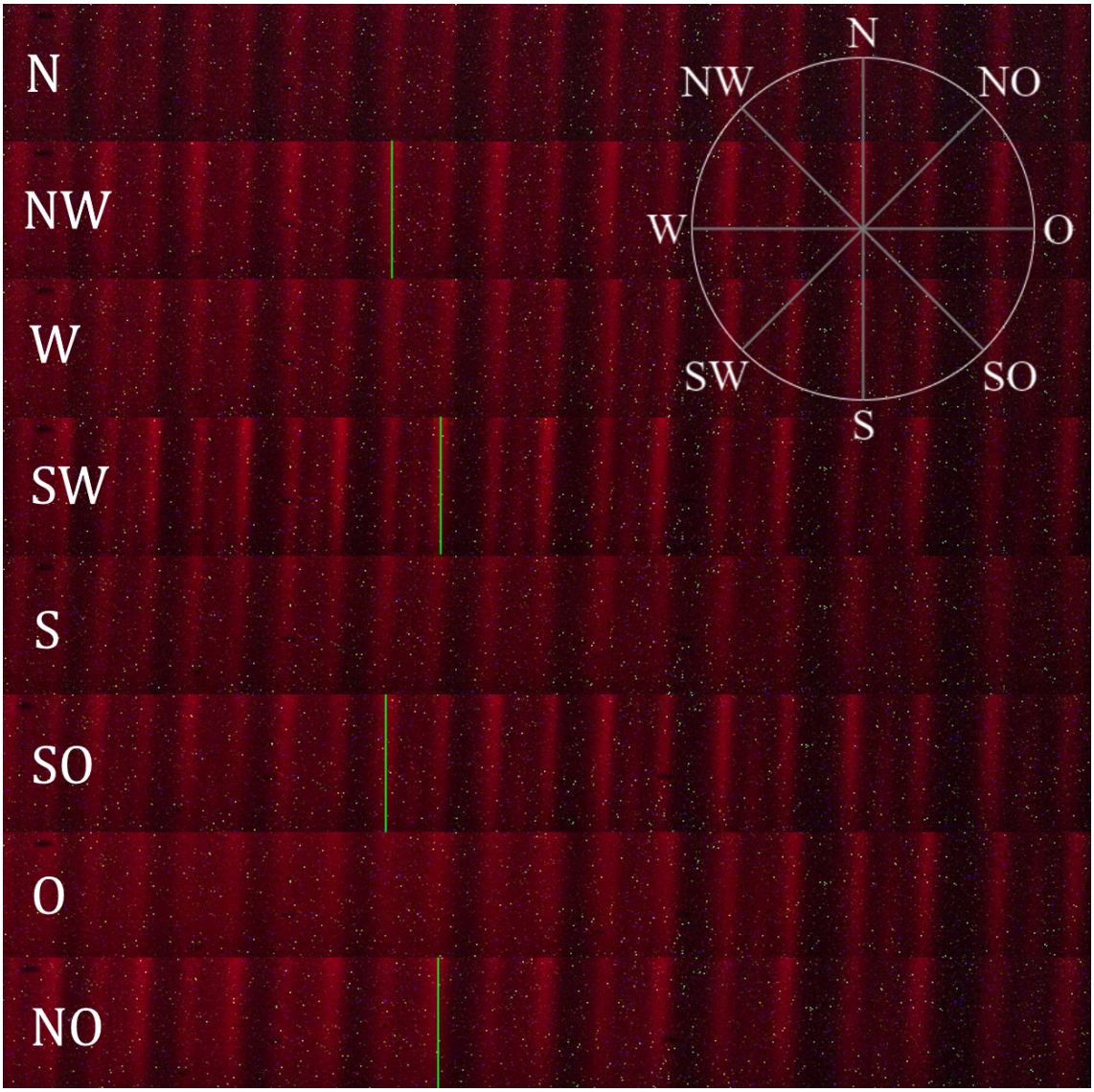

Figure 9: The effect of applying a $\lambda/4$ waveplate **and** a linear polarisation filter to the longitudinal spectrum. The compass analogy indicates how the linear filter was turned for the different measurements

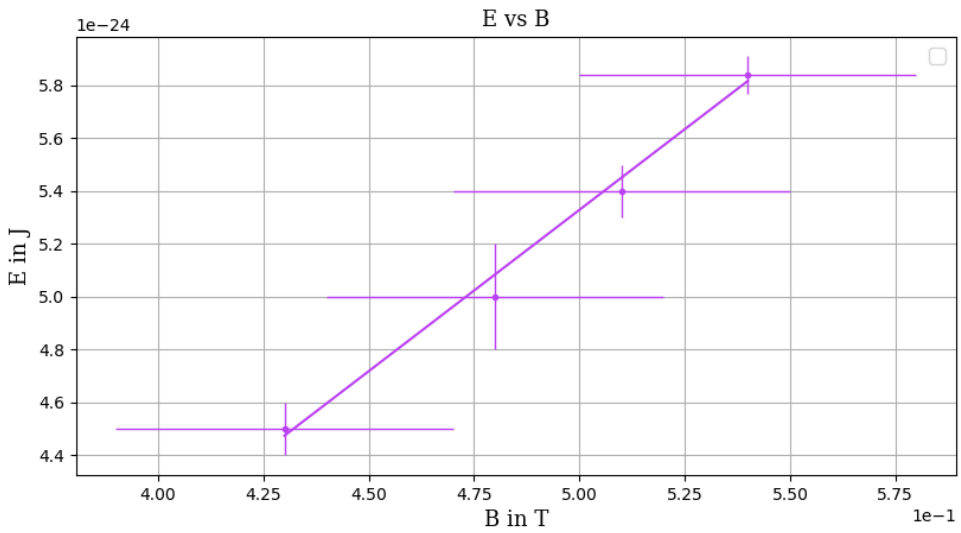

Figure 10: E versus B with a linear fit $E = aB + b$ with $a = (1.2 \pm 0.3) \times 10^{-23} J/T$ and $b = (-7.7 \pm 0.2) \times 10^{-25} J$

screens use polarisation filters to control the light that they emit and as a side effect of this only emit linearly polarised light. When we hold our filter so that its polarisation axis is perpendicular to this polarisation axis of the monitor light no light will pass through.

Figure 9 shows how the angle of the linear filter affects the observed spectrum. In theory there should be an angle α at which we can completely filter out the left line and an angle $\alpha + 90°$ at which the right line disappears. We did not manage to find this angle. However, one can see the that depending on the filter's position, one line becomes more prominent than the other and that this happens with a period of about 180°, as expected. Perhaps the $\lambda/4$ waveplate was damaged or perhaps we were not careful enough with sources of reflected light.

2.4 Measuring the Bohr magneton μ_B

We can use the images in figure 6 to find the pixel position of the π and σ lines of the different orders at different currents. Because of the geometry of the Lummer-Gehrcke plate we can use the relationship (see the experiment instructions for a detailed derivation)

$$\delta\lambda = \frac{\delta a}{\Delta a} \frac{\lambda^2}{2d\sqrt{n^2 - 1}} \tag{6}$$

where Δa is the distance between two orders of interference (= the distance between two π lines), δa is the distance between the line with wavelength λ and the line with wavelength $\lambda + \delta\lambda$ (= the distance between a π line and the σ lines), $n = 1.4567$

is the relevant refraction index and $d = (4.04 \pm 0.01)mm$ is the thickness of the Lummer-Gehrcke plate. See part II for how we determined λ. For the uncertainty we find

$$\delta\lambda_{err} = \delta\lambda\sqrt{(\frac{a_{err}}{a})^2 + (\frac{d_{err}}{d})^2} \tag{7}$$

with $a = \frac{\delta a}{\Delta a}$ and $a_{err} = a\sqrt{(\delta a_{err}/\delta a)^2 + (\Delta a_{err}/\Delta a)^2}$. Now the energy shift between the π line and the σ line is

$$E = hc(\frac{1}{\lambda} - \frac{1}{\lambda + \delta\lambda}) \tag{8}$$

and

$$E_{err} = hc\frac{\delta\lambda_{err}}{(\lambda + \delta\lambda)^2} \tag{9}$$

where h is Planck's constant and c is the speed of light. The Bohr magneton is simply

$$\mu_B = E/B \tag{10}$$

with $\mu_{Berr} = \mu_B\sqrt{(\frac{E_{err}}{E})^2 + (\frac{B_{err}}{B})^2}$ (see (5)). B is the magnetic field strength for which we can use the results of the hysteresis measurements.

To find a, we need to go through the images in figure 6 and label all the lines. As noted before, our images are quite fuzzy and there was some sort of background signal that needed to be filtered out. After that, we used a superposition of three Gaussian peaks to fit each diffraction order. Figure 11 shows what these steps look like on our data for $I = 12A$.

We calculated the Bohr magneton for four different currents. The average was

$$\mu_B = (1.4 \pm 0.2) \times 10^{-23} J/T$$

We can also plot the different values for E and B like in figure 10. Now μ_B is given by the slope. We find

$$\mu_B = (1.2 \pm 0.3) \times 10^{-23} J/T$$

See chapter 4 for a discussion of these values.

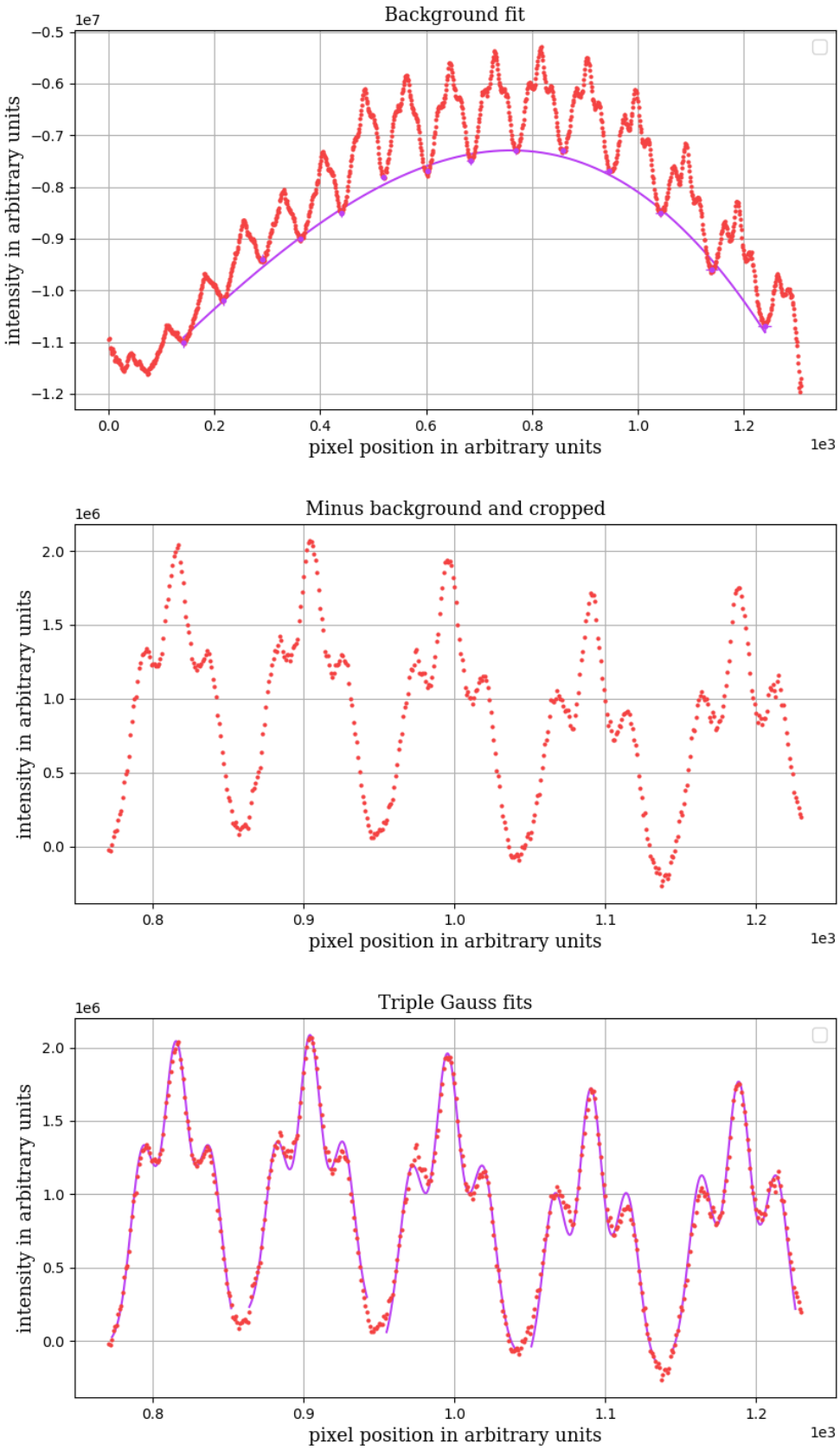

Figure 11: The three steps to finding the location of the lines, demonstrated on the data for $I = 12A$. The data was cropped to make the triple Gauss fit more visible for this demonstration.

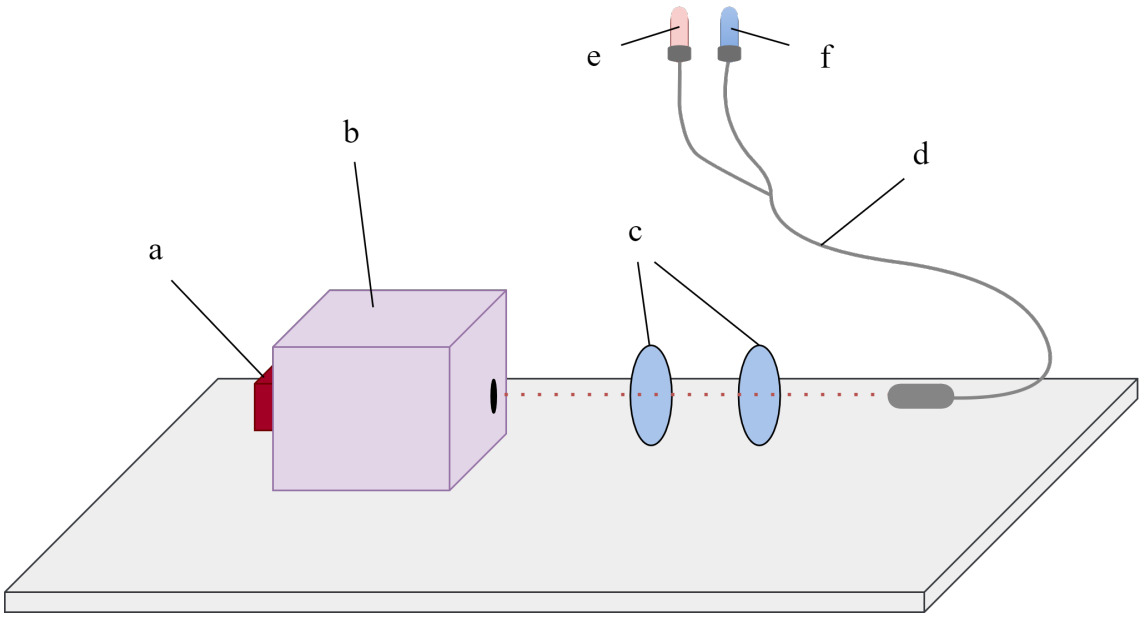

Figure 12: Simplified experimental setup. a) Camera b) Spectrometer c) Lenses d) Light guide e) Neon lamp f) Cadmium lamp

3 PART II: Precision spectroscopy

3.1 Setup

In this part, we want to measure the wavelength of a red spectral line of cadmium at about $\lambda \approx 645nm$. Figure 12 shows our experimental setup. We use a Y-shaped light guide to superimpose the light from the neon and the cadmium lamp. The lenses then focus the light into a Czerny-Turner spectrometer whose output we observe through a camera.

3.2 Dispersion function of the spectrometer

First we need to find the dispersion function of the spectrometer that we are using. Figure 13 shows the superimposed spectrum of cadmium and neon. The leftmost and the two rightmost lines are from neon and we know where we expect those. So we can use those three peaks to find the relationship between the pixel location and the actual wavelength in nm. Figure 14 shows what this fit looks like. We can see that for one picture with only three data points, a linear fit is completely adequate. For this part and later ones, all spectral lines are fitted with Gauss curves. This is because the shape of the spectral line is dominated by Doppler broadening. At some temperature $T > 0K$ the velocities of the cadmium atoms will follow a Maxwell-Boltzmann distribution which is Gaussian shaped. The light from atoms that are

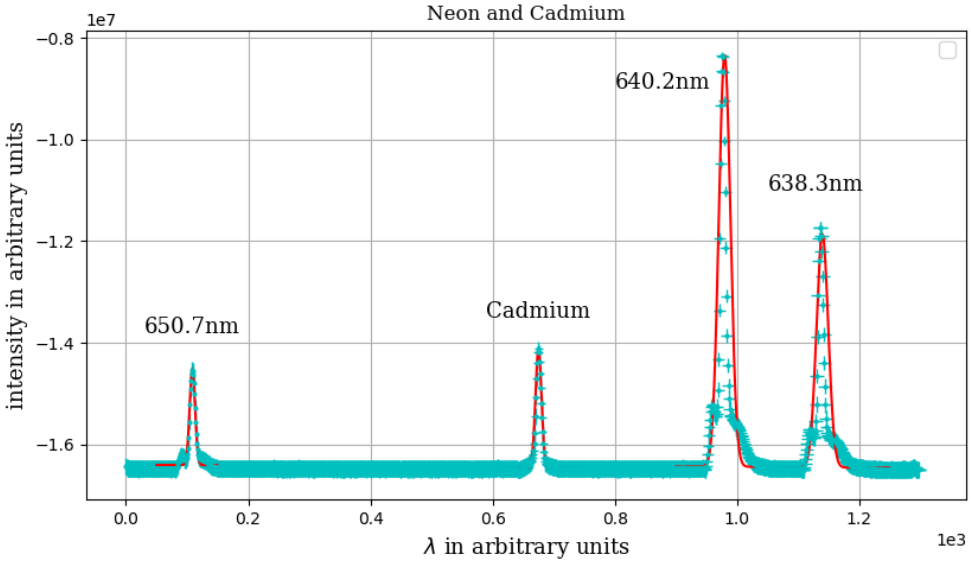

Figure 13: Superposition of the neon and the cadmium spectrum with Gauss fits at the peak locations.

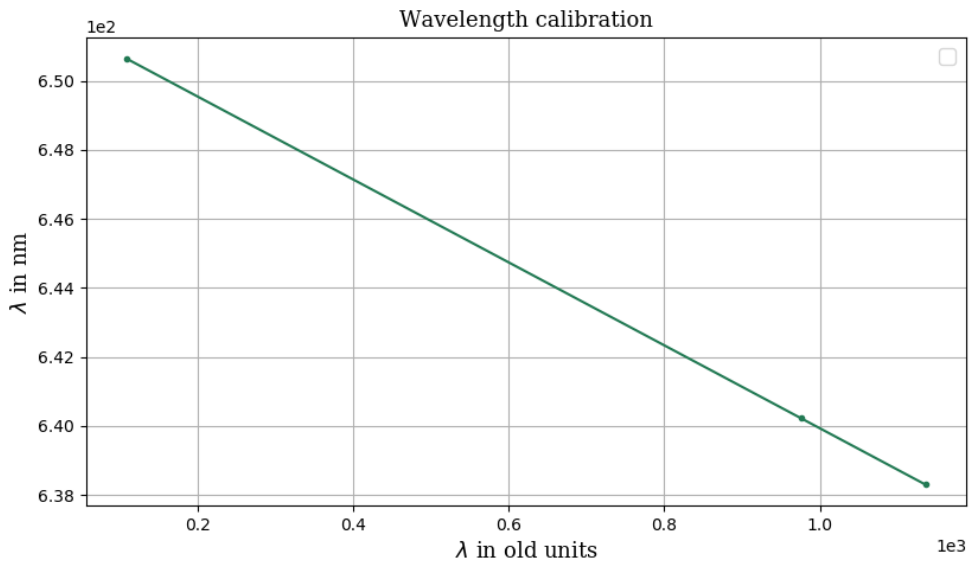

Figure 14: We use the neon lines from figure 13 to find the relationship between the pixel location and the wavelength in nm. The fit function is $x_{\text{new units}} = a * x_{\text{old units}} + b$ with $a = (-1.2022 \pm 0.0001) \times 10^{-2}\, nm$ and $b = (6.519572 \pm 0.000002) \times 10^{2}\, nm$.

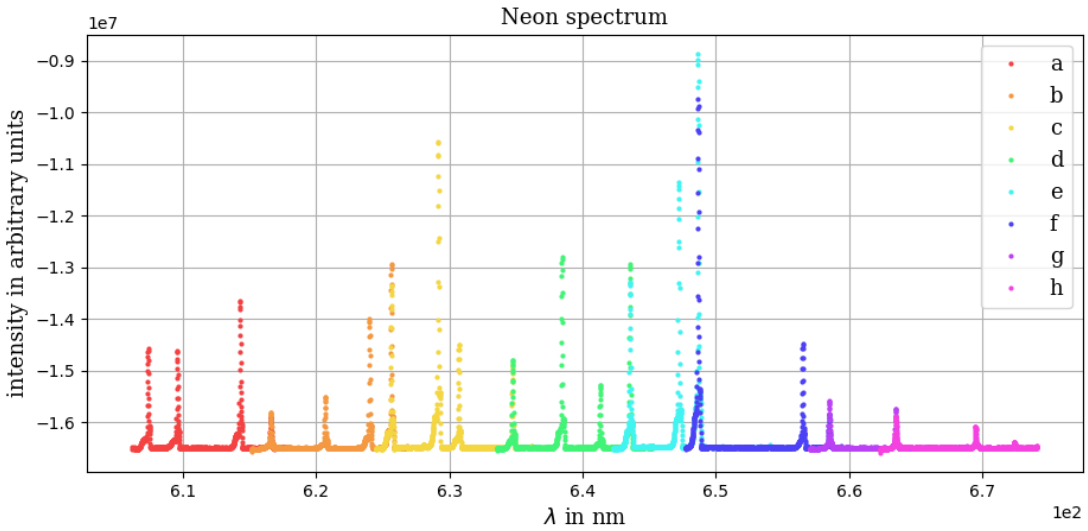

Figure 15: The neon spectrum. Each letter and colour indicates a different measurement. By cross-referencing the spectral lines we confirmed that our wavelength axis is skewed and should not be used for quantitative measurements.

moving away from the camera will be redshifted and the light from atoms that are moving towards us will be blueshifted. The redshift grows linearly with the velocity (for small speeds) and so the redshift will also be shaped like Gaussian.

3.3 Cadmium line

Now we can rescale the λ axis in figure 13 to nm and determine the position of the cadmium line. We find

$$\lambda = (643.85 \pm 0.02)nm$$

with a simple Gaussian fit. See chapter 4 for a discussion of this value.

3.4 Neon spectrum

We now want to try to take a picture of the red part of the neon spectrum. To do this we start by taking an image of the two orange lines and then work our way to longer wavelengths, one picture at a time. By making sure that any two consecutive pictures have a line in common, we can stitch the pictures together. Figure 15 shows the result of this. Note that the colours are only indicative of the measurement and not of the actual colour of the spectral line. All of these lines are orange or red. See chapter 4 for a comparison with reference values.

4 Discussion and Conclusion

4.1 Discussion of Part I

We started by finding the relationship between the current in the electromagnets I and the induced magnetic field B. We found that the cores exhibit hysteresis but that a linear fit over the average values of B worked well too. In later measurements we used these average values, mainly because we did not note down whether we were increasing or decreasing the current during those measurements. If we had wrote that down, we could have used the more appropriate value for the magnetic field and increased the accuracy of our derived value for μ_B. See more on that part below.

In the next part we observed the red cadmium line and its splitting when an external magnetic field is applied. We found that the splitting increases with the magnetic field strength and we were able to confirm the predictions of the transition dipole moment about the polarisation of the light. However, the image quality of our measurements was very poor and required many hours of post-production to become presentable. The lenses and filters had smudges and scratches on them and the $\lambda/4$ waveplate did not seem to work well (see figure 9). Perhaps a protective glass would prevent further damage to the waveplate.
By fitting the pixel position of the σ and π lines we derived the energy splitting which together with the magnetic field strength gave us a value for the Bohr magneton. We did this for four different values of B and took the average:

$$\mu_B = (14 \pm 2) \times 10^{-24} J/T$$

We also plotted the four different values for E and B and determined μ_B via the slope:

$$\mu_B = (12 \pm 3) \times 10^{-24} J/T$$

The real value is $\mu_B = 9.27 \times 10^{-24} J/T$. This is within 3σ and 1σ of our measurements, respectively. Our measurement was successful. However, our relative errors are quite large and the literature value does lie outside of 2σ of our first measurement, so we should look into sources of uncertainty and systematic errors.
An important part of this measurement is finding the location of the lines on the camera images. This took a lot of time and effort because of the poor quality of the images. The last image in figure 11 shows our best five fits. Those yielded positions with relative errors of less than 5% but most of our fits were much worse than that. Especially for smaller line separations at weaker magnetic fields it often took tens

of thousands of iterations for the Python fit to converge. This is a major source of uncertainty and could only be reduced by using better equipment.
Another source of error is the magnetic field strength. It was quite hard to put the Hall probe where the cadmium lamp would sit later. If we were too far away with the probe we would have measured a weaker field than the cadmium lamp would actually experience. This in turn could explain why our Bohr magneton was consistently measured too big as $\mu_B \propto 1/B$ (see (10)).

4.2 Discussion of Part II

In the second part we superimposed the spectra of neon and cadmium to find the wavelength of the red cadmium line that we used in the first part. We managed to get an image where the cadmium line appeared next to three neon lines whose wavelengths we were given. We found that for these three lines, a linear fit was almost perfect (see the relative errors in figure 14). We used this to rescale the λ axis in our superposition image and found the cadmium line at

$$\lambda_{exp} = (643.85 \pm 0.02)nm$$

`physics.nist.gov` puts the cadmium line at

$$\lambda_{reference} = 643.847nm$$

which is within 1σ of our measurement. The relative error could be reduced further by for example working at lower temperatures (to reduce Doppler broadening of the lines), with a better camera (to increase the resolution of our images) or with a more precise calibration.

We then tried to take a picture of an extract of the neon spectrum by stitching together images that have one spectral line in common. Figure 15 shows the resulting spectrum. We compared these lines to the literature and even though we could manually identify most spectral lines by their relative distance and intensity, their absolute location was usually off by some nm. We think that this is because our assumption of a linear dispersion curve is too strong. We tried to refit the spectrum with new calibrations but it was not possible to linearly transform the spectrum to fit the reference values. Another possibility is that we simply missed a line or overwrote a picture so that parts of the spectrum are shifted. However, we could not identify such a point.

4.3 Conclusion

We were able to convince ourselves of all qualitative predictions that quantum physics makes about the red spectral line of cadmium at $644nm$ and we managed to determine its wavelength with a relative error of only about 3×10^{-5}. So we can call it a successful experiment.
However, the quantitative measurement in the first part were quite imprecise and could be improved by a more precise measurement of the magnetic field and by using a camera with a higher resolution.